Microstructures and mechanical properties of pure tantalum processed by high-pressure torsion

2014 IOP Conf. Ser.: Mater. Sci. Eng. 63 012100

(http://iopscience.iop.org/1757-899X/63/1/012100)

IOP Conf. Series: Materials Science and Engineering **63** (2014) 012100 doi:10.1088/1757-899X/63/1/012100

Microstructures and mechanical properties of pure tantalum processed by high-pressure torsion

Y Huang[1], N Maury[2], N X Zhang[1] and T G Langdon[1,3]

[1]Materials Research Group, Faculty of Engineering and the Environment, University of Southampton, Southampton SO17 1BJ, UK
[2]École Nationale Supérieure des Ingénieurs en Arts Chimiques et Technologiques (ENSIACET), National Polytechnic Institute of Toulouse (INPT), 31077 Toulouse CEDEX 04, France
[3]Departments of Aerospace & Mechanical Engineering and Materials Science, University of Southern California, Los Angeles, CA 90089-1453, USA

E-mail: y.huang@soton.ac.uk

Abstract. A body-centred cubic (BCC) structure metal, tantalum, was processed by high-pressure torsion (HPT) at room temperature with different numbers of rotations. The microstructural evolution was studied by electron backscatter diffraction (EBSD). The grain sizes were significantly refined at the disk edge area in the early stages of deformation (N = 0.5) but tended to attain saturation after the numbers of rotations was increased to N = 5. As the deformation continued, some coarse grains appeared in the disk edge areas and it appeared that there was structural recovery at the expense of grain boundary migration in the tantalum during HPT processing. Microhardness measurements showed the hardness gradually evolved towards a more homogenized level across the disk surfaces as the numbers of rotations increased. The hardness level after N = 10 turns was slightly lower than after N = 5 turns, thereby indicating the occurrence of a recovery process after 5 turns.

Keywords: Electron backscatter diffraction; Grain size; Hardness; High-pressure torsion; Tantalum

1. Introduction

Tantalum is a refractory metal having excellent room-temperature ductility (greater than 20% tensile elongation) [1]. Because of its unique corrosion properties (i.e. chemically inert), tantalum finds use in the chemical industry, particularly as valves, heat exchangers, and bayonet heaters [1, 2]. Tantalum is also highly bioinert and it is used as an orthopedic implant material [3]. The elasticity of tantalum makes it an appropriate material for hip replacements to avoid stress shielding [4]. Researchers are also considering using tantalum in prostheses instead of titanium. However, to make Ta comparable to Ti as an implant material, it is necessary to improve the material strength. According to the Hall-Patch relationship, the grain size is the major microstructural parameter dictating the properties of a polycrystalline material at room temperature. The traditional plastic working techniques (e.g. rolling, extrusion) for tantalum usually generate coarse grain microstructures. Therefore it is expected that ultrafine or nanostructured tantalum will have improved strength and enhanced performance.

Ultrafine or nanostructured materials can be produced through the application of severe plastic deformation (SPD) to conventional coarse-grained metals and typically the grain sizes are within the submicrometer or even the nanometer range [5]. Among various newly developed SPD techniques, equal-channel angular pressing (ECAP) [6] and high-pressure torsion (HPT) [7] are the most popular and successful processing methods. Processing by HPT is especially attractive because it leads to grains which are generally smaller than those produced using ECAP. In practice, ECAP and HPT have been successfully applied to various metals and alloys mainly having face-centered cubic (FCC) and hexagonal close-packed (HCP) crystal structures, for example, Al, Cu, Ni, etc. (FCC) and Mg, Ti, Zr, Zn etc. (HCP). The applications of SPD processing to body-centered cubic (BCC) metals and alloys are rather few. Only in recent years are there some reports on HPT processing of BCC crystal structure materials: for example, Nb [8-11], Cr [11, 12], W [13], Fe [14, 15], V and Mo [16] and Ta [17-19].

The limited research related to HPT processing of Ta available to date is based on studying the post-HPT deformation mode which includes the localized plastic deformation via shear bands for nanocrystalline Ta in compression [17] and adiabatic shear banding of high strain rate behavior in a Kolsky bar system [18]. A recent study examined the laser induced compression for post-HPT monocrystalline Ta [19]. Nevertheless, there have been no systematic studies on the HPT processing, the evolution of microstructure and the mechanical properties of tantalum.

In order to address this deficiency, the present research was initiated to provide a systematic study of the microstructure and mechanical property evolution in tantalum under high pressure conditions. Using these results, the overall objective was to establish procedures for enhancing the bio-applications of this material.

2. Experimental materials and procedures

The as-received Ta rod was 10 mm in diameter and it was received in an annealed state and having a purity of 99.9%. The tantalum rod was sliced into discs with thicknesses of ~1.2 mm and these discs were ground with abrasive papers to final thicknesses of ~0.8 mm in order to undertake HPT processing.

The discs were processed by HPT under quasi-constrained conditions [20, 21] through total numbers of turns, N, of 0.5, 1, 2, 5 and 10 at room temperature using an imposed pressure of 6.0 GPa and a rotational speed for the lower anvil of 1 rpm.

Following HPT processing, both an as-received sample and the HPT-processed discs were hot-mounted in bakelite and ground with abrasive papers. A final polishing was performed using a colloidal silica solution in order to achieve a mirror-like surface. For the as-received sample, the polished surface was etched by an ASTM 163 etchant. This etchant contains 30 mL of water (H_2O), 30 mL of sulfuric acid (H_2SO_4), 30 mL of hydrofluoric acid (HF) and 3 to 5 drops of 30% hydroxide peroxide (H_2O_2). The sample was immersed in the etchant for 20 to 40 seconds. Then the sample surface was observed in dark field mode using an Olympus BX51 optical microscope in order to determine the initial grain structure. The grain size was measured using the linear intercept method with Image J software. The grain structures in the HPT-processed samples were examined by electron backscattered diffraction (EBSD) using a JSM6500F thermal field emission scanning electron microscope (SEM).

The values of the Vickers microhardness, Hv, were measured on the polished surfaces and at positions along the disc diameters separated by incremental distances of 0.3 mm. The hardness measurements were taken using an FM300 hardness tester equipped with a Vickers

indenter with a load of 300 gf and a dwell time of 15 s. These measurements were used to give the variation of Hv across each disc diameter.

3. Experimental results

The microstructure of the as-received Ta is shown in Fig. 1. This material was in an annealed state with relatively coarse grains. The average grain size was measured as ~60 μm and the average hardness was ~87 Hv.

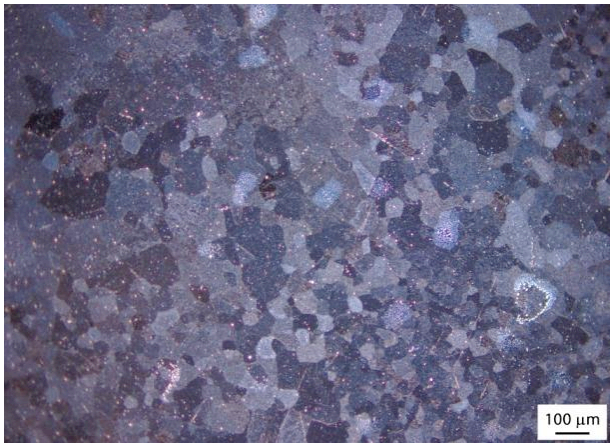

Fig. 1 Microstructure of as-received tantalum

3.1 Microstructure development during HPT processing

Representative microstructures during HPT processing are presented in Fig. 2 which includes both the centre and edge areas after 0.5 and 10 turns. The colours in Fig. 2 denote different grain misorientations as depicted in the unit triangles. In this EBSD mapping, high-angle grain boundaries (HAGBs) with misorientations greater than 15° are shown in thicker black lines and the thinner golden lines represent low-angle grain boundaries (LAGBs). As shown in Fig. 2(a), after 0.5 turn the disc edge area has experienced significant grain refinement and the grain size is reduced from ~60 μm in the as-received state to ~0.2 μm. Whereas Fig. 2(b) shows that the disc centre retains a coarse grain structure which is similar to the as-received condition and within the grains there are many sub-boundaries (golden lines) which were introduced by the HPT processing. The microstructures after 1 and 5 turns are not included in Fig. 2 but there was further grain refinement at the disc edge with increasing numbers of turns and the average grain sizes were ~0.16 and ~0.14 μm for 1 and 5 turns, respectively. When the number of turns increased to 10 in Fig. 2 (c) and (d), the microstructures became uniform from the edge to the centre with an average grain size of ~0.16 μm. However, it is also apparent from Fig. 2 (c) that some coarser grains appeared in the edge area.

The misorientation distributions after HPT processing are displayed in Fig. 3 where the angles >15° are high-angle boundaries. It should be mentioned that the misorientation distributions obtained in Fig. 3 are the pixel-to-pixel misorientation distributions, not the grain-to-grain misorientation distributions [22]. After 0.5 turn in Fig. 3 (a), the disc centre has a small fraction of high-angle boundaries (~22%) whereas the disc edge has a high fraction (~53%). Since the disc edge is subjected to a higher torsional strain than the centre, this leads to a higher fraction of high-angle boundaries. In Fig. 3 (b) after 10 turns of HPT, the centre and edge have similar number fractions of high-angle boundaries (~59% and ~61%).

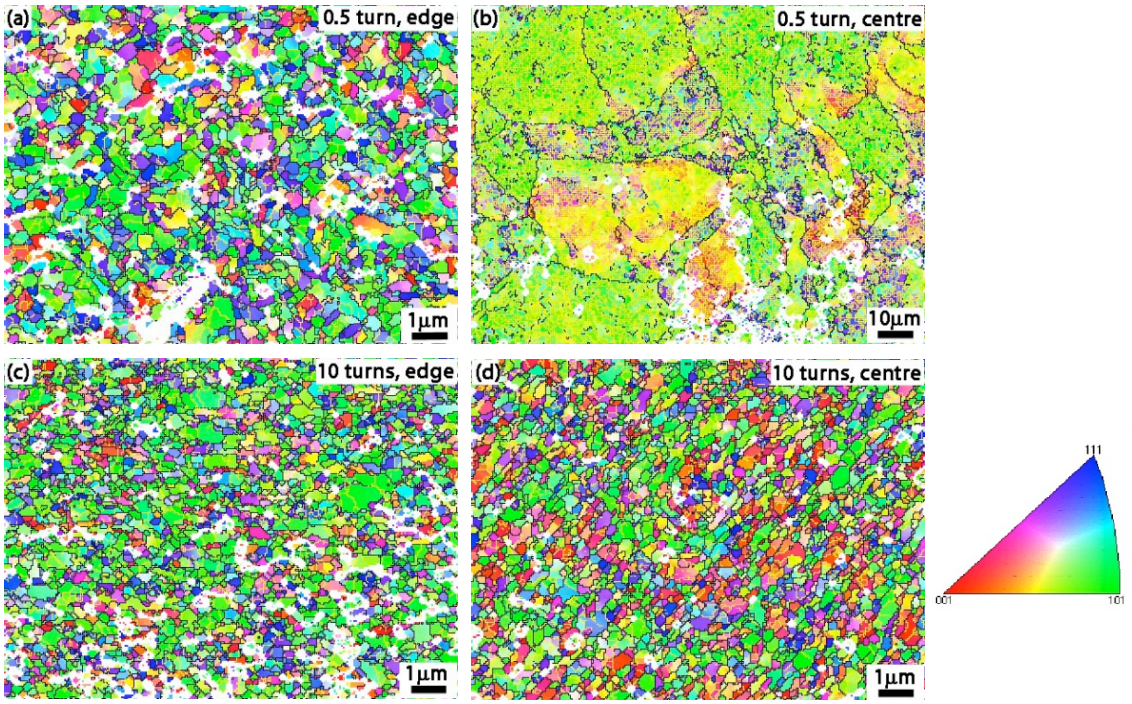

Fig. 2 Microstructures after HPT processing at disc edge and centre areas after (a, b) 0.5 and (c, d) 10 turns

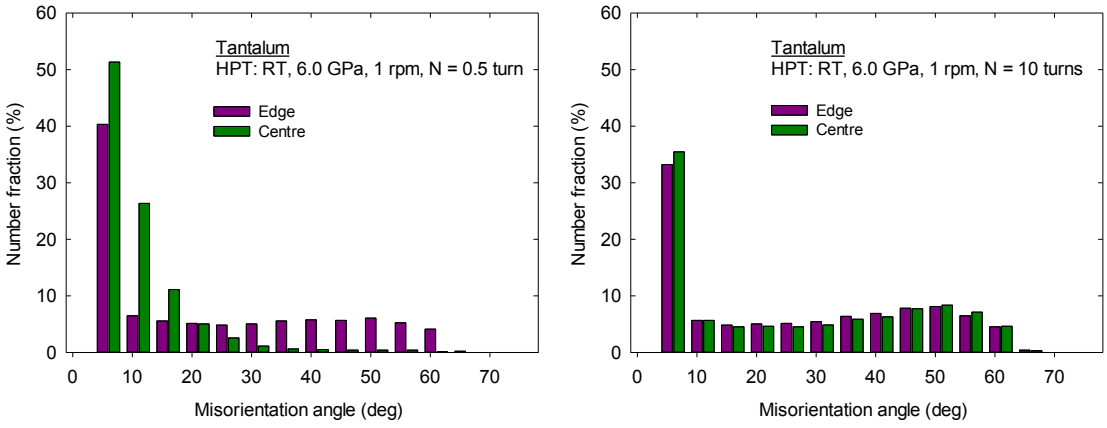

(a) (b)

Fig. 3 Misorientation distributions after HPT processing at disc edge and centre areas after (a) 0.5 and (b) 10 turns

3.2 Hardness evolution during HPT processing

The hardness evolutions with different number of turns during HPT processing are shown in Fig. 4. After 0.5 turn, the disc centre has the lowest hardness value, and the hardness increases almost linearly from the centre to the edge and reaches a maximum value at the edge. After 1, 2 and 5 turns, the patterns of the hardness distributions along the diameters change. The disc centre has the lowest hardness value and the hardness values increase from the centre to a

medium position to attain a saturation level and thereafter a saturation is maintained from the medium point to the disc edge. As shown in Fig. 4, the position the hardness attains the saturation plateau gradually moves towards the disc centre with increasing numbers of rotations. After 10 turns, although the hardness saturation plateau has extended almost to the disc centre area, the central hardness has not fully attained the saturation level but this value has increased significantly compared to the centre hardness values after 0.5, 1, 2 and 5 turns. Thus a more homogeneous hardness distribution is attained after 10 turns but nevertheless the overall hardness is slightly lower than the hardness value at the disc edge after 5 turns.

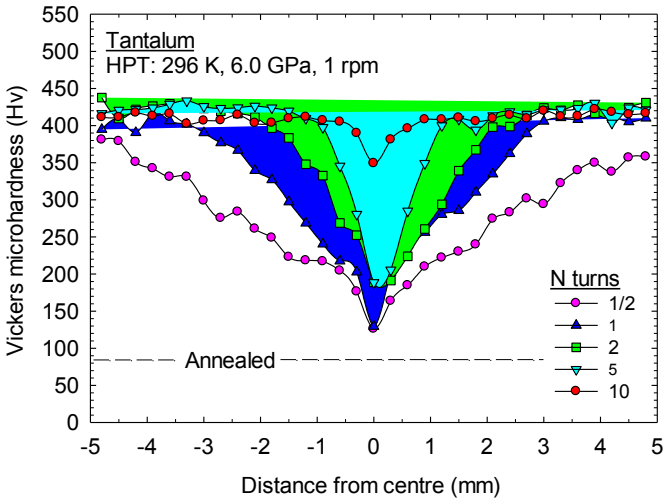

Fig. 4 Distribution of Vickers microhardness, Hv, along the diameter of discs processed by HPT for 0.5, 1, 2, 5 and 10 turns

4. Discussion

In FCC metals, slip generally occurs on {111} planes in <110> directions. The perfect Burgers vector is a/2<110>, which is a close-packed direction and represents the shortest repeat length in the crystal. The slip planes {111} have the largest interplanar spacing of those containing close-packed directions. In the case of BCC metals, slip is more complex. It is clear from numerous experiments [23] that slip generally occurs in the closest packed <111> direction and the Burgers vector is a/2<111>. The planes with the largest interplanar spacing are {110} followed by {112} then {123}. Examining Fig. 2, there are many green-coloured grains representing grains having their {110} plane parallel to the disc surface and some pink-coloured grains representing grains having {112} planes parallel to the disc surface. In Fig. 2 (a) and (c), it is shown that the fraction of blue-coloured grains is reduced with increasing numbers of rotations in the disc edge area. Since the torsion strain is applied in a direction parallel to the disc surface, therefore it is reasonable to conclude that slip in Ta occurs on {110} and {112} planes to accommodate the severe torsional strain.

Figure 2 demonstrates that significant grain refinement is attained in both the disc edge and centre area after 10 turns. Observations and measurements show the grain size tends to attain saturation at the disc edge area after N = 5 turns. As the numbers of rotations increased to 10 turns, no further grain refinement was observed in the disc edge area. A similar result was reported in HPT processing of Niobium [9] and there was an assumption

that structures recover at the expense of grain boundary migration [10]. There is also the possibility of texture induced grain coalescence, which means when several grains with similar orientations come together and join, the boundaries between them become new low-angle boundaries and the merging of the grains leads to the generation of a new coarser structure. Tantalum has a relatively high stacking fault energy [24], thereby facilitating the movement of dislocations within its crystal structure. In this respect, tantalum is similar to many FCC metals.

It has been established in HPT that the equivalent von Mises strain, ε, may be estimated using the relationship [25-27]

$$\varepsilon = \frac{2N\pi r}{h\sqrt{3}} \tag{1}$$

where r and h are the radius and height (or thickness) of the disc. It follows from eq. (1) that the strain is zero at the centre of the disc and reaches a maximum value at the outer edge. The present results in Fig. 4 demonstrate that at an early stage deformation after 0.5 turn the hardness varies linearly with the disc radius from the centre to the edge. As the number of turns increases to 1, the hardness displays a two-stage behaviour which includes a linear variation and a saturation plateau. The proportion of hardness in the linear region decreases with numbers of rotations whereas the proportion of saturation plateau increases with numbers of rotations. The hardness reaches a reasonably homogenous level across the disc diameter after 10 turns. The hardness at the centre of the disc gradually increases with the numbers of rotations although it does not attain the saturation level after 10 turns. The hardness at the edge of disc after 10 turns is slightly lower than that after 5 turns. Fig. 2 (c) shows that some coarse grains appear in the edge area after 10 turns and these coarse grains probably account for the slight drop in the overall hardness after 10 turns.

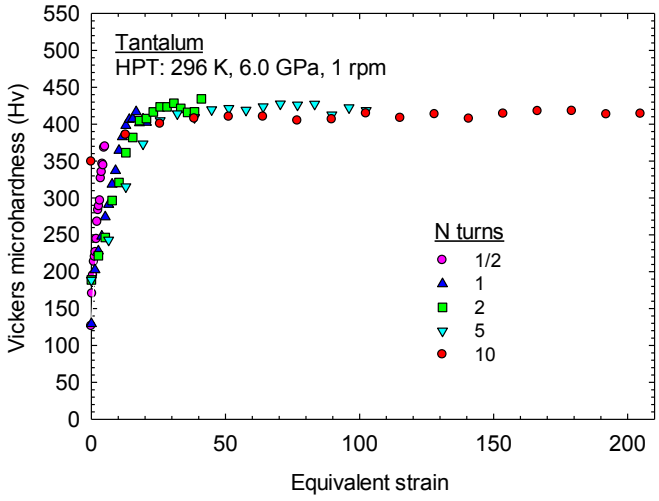

Fig. 5 Values of the Vickers microhardness plotted as a function of the equivalent strain in discs processed by HPT for 1/2, 1, 2, 5 and 10 turns

Several reports have shown that the variations in hardness across HPT discs may be readily correlated at every point by plotting the hardness values against the equivalent strain using equation (1) [28]. To evaluate the hardness variation vs equivalent strain in the metal

Ta, the values of the Vickers microhardness are plotted as a function of the equivalent strain in Fig. 5 using data from Fig. 4 where these hardness values were obtained by averaging the two sets of measurements recorded on either side and equidistant from the centres of the discs. Inspection of Fig. 5 shows that after 1 turn the disk hardness tends to attain a saturation level near the edge area whereas after 2, 5 and 10 turns the disc centre areas have not fully achieved the saturation level. The hardness saturation level in Ta is ~430 Hv.

The plot in Fig. 5 is typical of many materials and they correspond to HPT processing in the absence of any significant recovery [29-31]. The recovery observed in the 10 turns sample may be related to structural recovery which occurs at the expense of grain boundary migration.

5. Summary

HPT provides a valuable processing route for attaining homogenous grain refinement and a strength improvement in tantalum. In HPT processing of tantalum, slip occurs in {110} and {112} planes to accommodate severe torsional strain. Tantalum shows recovery and some coarser grains at higher numbers of rotations.

Acknowledgement

This work was supported by the European Research Council under ERC Grant Agreement No. 267464-SPDMETALS.

References

[1] Buckman Jr R W 2000 *JOM* **52** (3) 40
[2] Blake C W 1935 *Industrial and Energy Chemistry* **27** 1166
[3] Matsuno H, Yokoyama A, Watari F, Uo M and Kawasaki T 2001 *Biomater.* **22** 1253
[4] Black J 1994 *Clinical Mater.* **16** 167
[5] Huang Y and Langdon T G 2013 *Mater. Today* **16** 85
[6] Valiev R Z and Langdon T G 2006, *Prog. Mater. Sci.* **51** 881
[7] Zhilyaev A P and Langdon T G 2008, *Prog. Mater. Sci.* **53** 893
[8] Popova E N, Popov V V, Romanov E P and Pilyugin V P 2006 *Physics of Metals and Metallography* **101** 52
[9] Popova E N, Popov V V, Romanov E P and Pilyugin V P 2007 *Physics of Metals and Metallography* **103** 407
[10] Popov V V, Popova E N, Stolbovskii A V, Pilyugin V P and Arkhipova N K 2012 *Physics of Metals and Metallography* **113** 295
[11] Lee S and Horita Z 2012 *Mater. Trans.* **53** 38
[12] Wadsack R, Pippan R and Schedler B 2003 *Fusion Engineering and Design* **66-68** 265.
[13] Wei Q, Zhang H T, Schuster B E, Ramesh K T, Valiev R Z, Kecskes L J, Dowding R J, Magness L and Cho K 2006 *Acta Mater.* **54** 4079
[14] Edalati K, Fujioka T and Horita Z 2009 *Mater. Trans.* **50** 44
[15] Watanabe R 2006 *Mater. Trans.* **47** 1886
[16] Lee S, Edalati K and Horita Z 2010 *Mater. Trans.* **51** 1072
[17] Ligda J P, Schuster B E and Wei Q 2012 *Scripta Mater.* **67** 253
[18] Wei Q, Pan Z L, Wu X L, Schuster B E, Kecskes L J and Valiev R Z 2011 *Acta Mater.* **59** 2423
[19] Lu C H, Remington B A, Maddox B R, Kad, B, Park H S, Kawasaki M, Langdon T G and Meyers M A 2013 *Acta Mater.* **61** 7767

[20] Figueiredo R B, Cetlin P R and Langdon T G 2011 *Mater. Sci. Eng.* A **528** 8198
[21] Figueiredo R B, Pereira P H R, Aguilar M T P, Cetlin P R and Langdon T G 2012 *Acta Mater.* **60** 3190
[22] Tóth L S, Beausir B, Gu C F, Estrin Y, Scheerbaum N, Davies C H J 2010 *Acta Mater.* **58** 6706
[23] Weinberger C R, Boyce B L and Battaile C C 2013 *Int. Mater. Rev.* **58** 296
[24] Ahlers M 1970 *Metall. Trans.* **1** 2415
[25] Valiev R Z, Ivanisenko Yu V, Rauch E F and Baudelet B 1996 *Acta Mater.* **44** 4705
[26] Wetscher F, Vorhauer A, Stock R and Pippan R 2004 *Mater. Sci. Eng. A* **387–389** 809
[27] Wetscher F, Pippan R, Sturm S, Kauffmann F, Scheu C and Dehm G 2006 *Metall. Mater. Trans. A* **37** 1963
[28] Vorhauer A and Pippan R 2004 *Scripta Mater.* **51** 921
[29] Kawasaki M, Ahn B and Langdon T G 2010 *Acta Mater.* **58** 919
[30] Kawasaki M, Ahn B and Langdon T G 2010 *Mater. Sci. Eng. A* **527** 7008
[31] Kawasaki M 2014 *J. Mater. Sci.* **49** 18